Eur J Nucl Med Mol Imaging (2012) 39:309–315
DOI 10.1007/s00259-011-1940-8

ORIGINAL ARTICLE

The significance of bremsstrahlung SPECT/CT after yttrium-90 radioembolization treatment in the prediction of extrahepatic side effects

Hojjat Ahmadzadehfar · Marianne Muckle · Amir Sabet · Kai Wilhelm · Christiane Kuhl · Kim Biermann · Torjan Haslerud · Hans-Jürgen Biersack · Samer Ezziddin

Received: 28 June 2011 / Accepted: 9 September 2011 / Published online: 6 October 2011

Abstract
Purpose Unwanted deposition of ^{90}Y microspheres in organs other than the liver during radioembolization of liver tumours may cause severe side effects such as duodenal ulcer. The aim of this study was to evaluate the significance of posttherapy bremsstrahlung (BS) SPECT/CT images of the liver in comparison to planar and SPECT images in the prediction of radioembolization-induced extrahepatic side effects.
Methods A total of 188 radioembolization procedures were performed in 123 patients (50 women, 73 men) over a 2-year period. Planar, whole-body and BS SPECT/CT imaging were performed 24 h after treatment as a part of therapy work-up. Any focally increased extrahepatic accumulation was evaluated as suspicious. Clinical follow-up and gastroduodenoscopy served as reference standards. The studies were reviewed to evaluate whether BS SPECT/CT imaging was of benefit.
Results In the light of anatomic data obtained from SPECT/CT, apparent extrahepatic BS in 43% of planar and in 52% of SPECT images proved to be in the liver and hence false-positive. The results of planar scintigraphy could not be analysed further since 12 images were not assessable due to high scatter artefacts. On the basis of the gastrointestinal (GI) complications and the results of gastroduodenoscopy, true-positive, true-negative, false-positive and false-negative results of BS SPECT and SPECT/CT imaging in the prediction of GI ulcers were determined. The sensitivity, specificity, positive and negative predictive values and the accuracy of SPECT and SPECT/CT in the prediction of GI ulcers were 13%, 88%, 8%, 92% and 82%, and 87%, 100%, 100%, 99% and 99%, respectively.
Conclusion Despite the low quality of BS images, BS SPECT/CT can be used as a reliable method to confirm the safe distribution of ^{90}Y microspheres and in the prediction of GI side effects.

Keywords Bremsstrahlung · SPECT/CT · Radioembolization · Liver tumours · Liver metastases

Introduction

Radioembolization (RE) with ^{90}Y microspheres is a promising catheter-based liver-directed modality for patients with primary and metastatic liver cancer. Overall, the incidence of complications for appropriately selected patients and meticulously targeted delivery is low [1]. Serious complications have been reported when excessive amounts of microspheres are inadvertently deposited in organs other than the liver or when the liver receives more radiation than its tolerance (called RE-induced liver disease) [2]. Reported complications include gastrointestinal (GI) ulceration/bleeding, gastritis/duodenitis, cholecystitis, pancreatitis, radiation pneumonitis and hepatic decompensation [3].

Hojjat Ahmadzadehfar and Marianne Muckle contributed equally to this work.

H. Ahmadzadehfar (✉) · M. Muckle · A. Sabet · K. Biermann · T. Haslerud · H.-J. Biersack · S. Ezziddin
Department of Nuclear Medicine, University Hospital Bonn, Sigmund-Freud-Str. 25, 53127 Bonn, Germany
e-mail: hojjat.ahmadzadehfar@ukb.uni-bonn.de

K. Wilhelm
Department of Radiology, University Hospital Bonn, Bonn, Germany

C. Kuhl
Department of Radiology, University Hospital Aachen, Aachen, Germany

It is recommended that RE is followed by a posttherapy bremsstrahlung (BS) scan to document the distribution of microspheres within the liver. However, until recently the quality of BS images acquired by nuclear medicine equipment only allowed an approximate verification of tracer distribution, but newly available hybrid SPECT/CT cameras enable direct correlation of anatomic and functional information. This has resulted in a better localization and definition of scintigraphic findings. However, there are only a few reports of the utility of BS images in the literature. Tehranipour et al. reported that planar ^{90}Y BS scintigraphy is able to demonstrate the distribution of ^{90}Y microspheres in liver metastases [4] while Sebastian et al. reported that planar BS imaging is able to demonstrate the delivery of resin microspheres to the target arterial territory despite being not accurate enough to rule out their distribution in other arterial territories close to the liver [5]. Furthermore, Mansberg et al. demonstrated tumour uptake of tracer in ^{90}Y BS SPECT/CT images in a patient undergoing RE [6].

The use of advanced reconstruction techniques, such as iterative reconstruction, may further improve image quality. Quantitative evaluation of BS scans with SPECT(/CT) indicates that this approach may be feasible despite scatter artefacts [2, 6–11]. At the moment there is no definitive method for BS acquisition and reconstruction parameters among the centres. In a recent phantom study, Ito et al. used three energy window widths of 50% (57–94 keV) centred at 75 keV, 30% (102–138 keV) at 120 keV, and 50% (139–232 keV) at 185 keV for BS acquisition set on the ^{90}Y BS spectrum [12]. It was found that the BS SPECT acquisition using the 120 keV window resulted in the highest resolution and the lowest uncertainty while the summed window (75, 120 and 185 keV) showed the highest sensitivity which was about three times higher than that of the 120 keV window.

The positive impact of SPECT/CT in diagnosing benign and malignant diseases has been shown in different studies [13–17]. Our aim was to evaluate the capability of BS SPECT/CT in the detection and localization of extrahepatic accumulation of ^{90}Y microspheres in comparison to that of planar and SPECT imaging and its value in the early prediction of RE-induced extrahepatic side effects. The significance of SPECT/CT with regard to intrahepatic distribution of ^{90}Y microspheres was not addressed in this study.

Materials and methods

Patients

A total of 188 RE procedures were performed in 123 patients with different types of cancer over a 2-year period (Table 1). The mean and median ages of the patients were 62 years and 64 years, respectively (range 26–89 years), and there were 50 women (41%) and 73 men (59%).

Table 1 Types of cancer in 123 patients who received RE therapy

Cancer	No. of patients	Percent
Colorectal cancer	40	32.5
Hepatocellular carcinoma	36	29.3
Neuroendocrine tumours	19	15.4
Breast cancer	11	8.9
Cholangiocellular carcinoma	8	6.5
Pancreatic carcinoma	3	2.4
Malignant melanoma	1	0.8
Ovarian cancer	1	0.8
Ocular melanoma	1	0.8
Lung sarcoma	1	0.8
Gastric cancer	1	0.8
Intestinal leiomyosarcoma	1	0.8

Pretreatment angiography and radioembolization

All patients underwent preparatory hepatic arteriography to define the vascular anatomy of the liver and to assess the vascularity of the hepatic tumour and metastases 1 to 3 weeks prior to the RE. This was combined with injection of ^{99m}Tc-macroaggregated albumin (^{99m}Tc-MAA) simulating the real therapy to rule out any shunting to the lung or GI tract. The patients received a whole-body ^{99m}Tc-MAA scan within 1 h of ^{99m}Tc-MAA injection followed by a SPECT scan (four patients) or a SPECT/CT scan (119 patients) of the abdomen. The angiographic procedure and the ^{99m}Tc-MAA scan has been described in detail in other reports by our group [17–19].

^{90}Y microspheres were injected after any new collateral vessels connecting to the GI tract had been ruled out by fluoroscopy in the therapy session. Of the RE procedures, 33 were performed as a whole-liver treatment in which the microspheres were injected separately into the right and left

Table 2 Anatomic location of extrahepatic ^{90}Y accumulation in SPECT/CT images

Location	No. of patients	Complications
Stomach	6	Yes
Duodenum	6	Yes
Intestine (other than duodenum)	1	Yes
Spleen	2	No
Abdominal wall	11	Yes (in only one patient)
Gallbladder	1	No

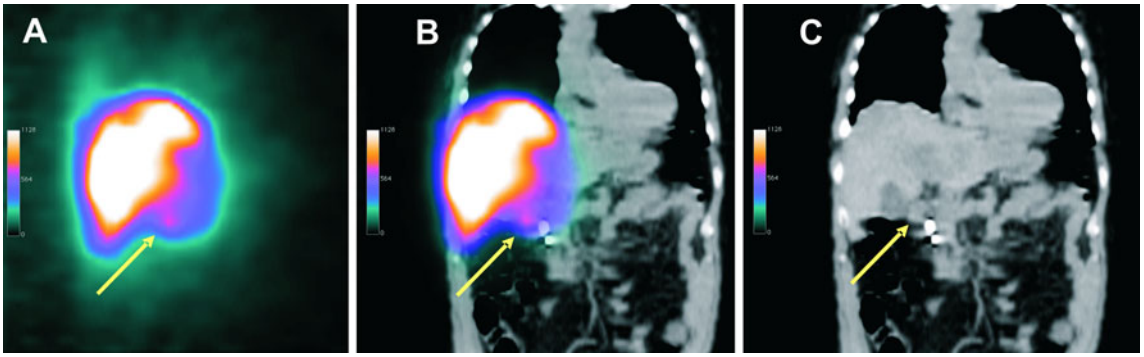

Fig. 1 A 67-year-old patient with colorectal cancer. Coronal BS SPECT (**a**), BS SPECT/CT (**b**) and CT (**c**) images. RE was performed with 1.10 GBq resin microspheres without any complications during delivery. A focally increased accumulation in the duodenum is apparent and was reported as suspicious for extrahepatic shunting of ^{90}Y (*arrows*). The patient received 40 mg daily pump inhibitor to reduce probable radiation-induced damage. The patient developed GI complaints 4 weeks after treatment. Gastroduodenoscopy showed a radiation-induced duodenal ulcer without active bleeding

hepatic arteries, 99 were performed for the right liver lobe, 45 were performed for the left liver lobe, and 11 were performed as superselective segmental therapies. The required activity for the treatment of each patient was calculated differently according to whether glass or resin microspheres were used. For the therapy with resin microspheres, the body surface area method was principally used, whereas for glass microspheres the defined dose-planning formula by Therasphere was used, which is dependent on a target dose and the patient's liver mass [20]. The dose calculation methods for both substances have been described previously in detail [2]. The mean and median administered doses were 1.86 GBq and 1.80 GBq, respectively (range 0.20-4.80 GBq).

Bremsstrahlung imaging

A whole-body scan followed by planar scintigraphy and SPECT/CT of the upper abdomen were performed in all patients within 24 h of RE. For BS acquisitions, a medium energy general purpose (MEGP) collimator was used with a very broad energy window of 55–250 keV to enhance the detection sensitivity of BS photons. For SPECT acquisitions a 128×128 matrix with 64 frames (20 s per frame) was used. Images were reconstructed using a Flash 3-D algorithm (Siemens) with eight iterations. The scan parameters for CT were 130 kV and 17 mAs with 5-mm slices.

Image interpretation

In all images the deposition of extrahepatic ^{90}Y microspheres was reviewed by two experienced nuclear medicine physicians using a Syngo workstation (VE25A; Siemens Healthcare). Images were read in the following order: planar, SPECT and SPECT/CT. In this study all BS images were assessed qualitatively without any quantification.

Reference standard

Follow-up including physical examination and laboratory testing was performed in all patients receiving RE on days 2, 30, 60 and 90 after the intervention and at 3-month intervals thereafter (if the patient was alive). All patients

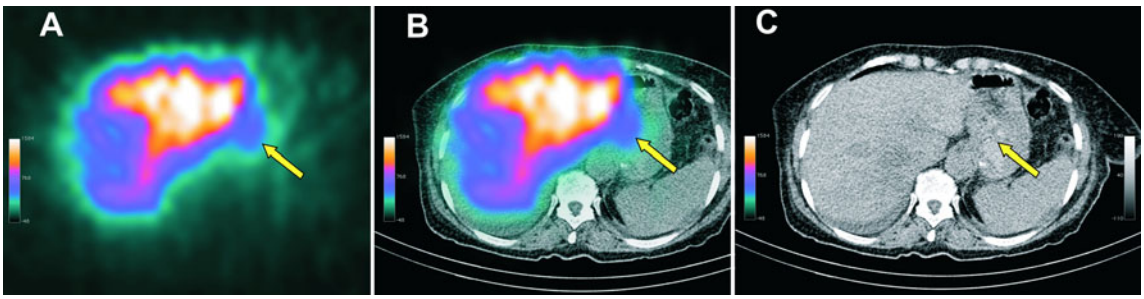

Fig. 2 A 75-year-old patient with cholangiocellular carcinoma received a whole-liver treatment with a total of 0.6 GBq ^{90}Y resin microspheres. Transverse BS SPECT (**a**), BS SPECT/CT (**b**) and CT (**c**) images. Microsphere delivery was ended because of stasis in both liver lobes, but without any backflow. During delivery the patient complained of nausea which was treated successfully with ondansetron. In the BS SPECT/CT image a diffusely increased gastric accumulation is apparent (*arrows*). The patient developed GI complaints 7 days after therapy due to a radiation-induced prepyloric ulcer in the antrum which was confirmed by gastroduodenoscopy

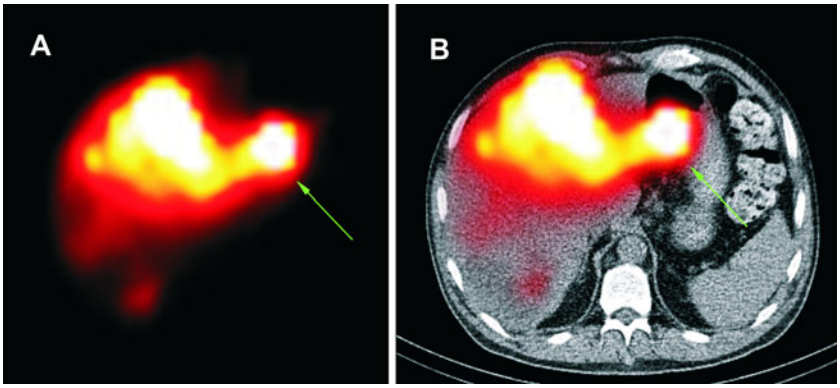

Fig. 3 Gastric accumulation of ^{90}Y microspheres (*arrows*) after RE with 3 GBq glass microspheres. Transverse BS SPECT (**a**), BS SPECT/CT (**b**) images. The patient developed severe GI bleeding 7 days after treatment

with GI complaints underwent gastroduodenoscopy and its results served along with the clinical follow-up as the reference standard.

Data analysis

Based on the reference standard, extrahepatic GI accumulations detected on planar, SPECT and SPECT/CT imaging were rated as true-positive (TP), true-negative (TN), false-positive (FP) or false-negative (FN). Sensitivity, specificity, positive predictive value (PPV), negative predictive value (NPV) and accuracy were calculated for all imaging modalities.

Results

Evaluating all 188 series of scans, an apparent extrahepatic BS was detectable in 11%, 17% and 12% of the planar, SPECT and SPECT/CT images, respectively. However, in the light of anatomic data obtained from SPECT/CT apparent extrahepatic BS in 43% of the planar and 52% of the SPECT images proved to be in the liver and hence FP. Furthermore, an exact anatomic localization of extrahepatic ^{90}Y microsphere accumulations was only possible by utilizing SPECT/CT (Table 2).

Prediction of GI ulcers

At least one suspect ^{90}Y accumulation in the GI region was detectable in SPECT images in 23 patients and SPECT/CT images in 13 patients.

The mean and median follow-up times were 8.4 and 6 months, respectively (range 2 – 32 months). Of the 123 patients, 27 developed mild to moderate GI complaints without any apparent GI bleeding 2 to 30 days after RE. In 9 patients a radiation-induced gastroduodenal ulcer was confirmed by gastroduodenoscopy (Figs. 1 and 2), whereas in the remaining 18 patients no pathology was found in the gastroduodenal region, and this was supported by later follow-up examinations. A further 7 patients developed severe GI complaints in the form of active GI bleeding 1 to 4 weeks after treatment, and in 4 of these a radiation-induced ulcer was established in gastroduodenoscopy (Fig. 3). The other 3 had had a history of gastric ulcer prior to RE, and there were no visible radiation-induced changes on gastroduodenoscopy.

According to the reference standard the numbers of TP, TN, FP and FN findings with BS SPECT and BS SPECT/CT imaging modalities were 2, 152, 21 and 13, and 13, 173, 0 and 2, respectively (Table 3). The results of planar scintigraphy were not compared with those of the two other modalities since 12 images (6.4%) were not assessable due to a high level of scatter artefacts. Altogether, truly diagnosed extrahepatic ^{90}Y accumulations indicating GI ulcers were identified in 1.1% of all studies by SPECT and in 6.9% by SPECT/CT.

The sensitivity, specificity, PPV, NPV and accuracy of SPECT and SPECT/CT in the prediction of GI ulcers were 13%, 88%, 8%, 92% and 82%, and 87%, 100%, 100%, 99% and 99%, respectively (Table 4). There was no significant correlation between the intensity of ^{90}Y microsphere accumulation and the severity of side effects.

^{90}Y microspheres in other abdominal organs and regions

^{90}Y microsphere accumulations were detected in the spleen, gallbladder and anterior abdominal wall in 2, 1 and 11 patients, respectively (Table 2). Tracer accumulation in the anterior abdominal wall indicating an open hepatic falciform artery was detected in 8 planar, in 9 SPECT and in 11 BS SPECT/CT images. The falciform ligament was seen in

Table 3 TP, TN, FP and FN of BS SPECT and SPECT/CT in the prediction of GI ulcers compared to the reference standard

	TP	TN	FP	FN
SPECT	2	152	21	13
SPECT-CT	13	173	0	2

Table 4 Sensitivity, specificity, PPV and NPV of BS SPECT and SPECT/CT in the prediction of GI ulcers

	Sensitivity, % (95% CI)*	Specificity, % (95% CI)*	PPV, % (95% CI)*	NPV, % (95% CI)†	Accuracy (%)
SPECT	13 (2–42)	88 (82–92)	8 (1–30)	92 (87–96)	82
SPECT/CT	87 (58–98)	100 (97–100)	100 (72–100)	99 (95–100)	99

*$P<0.0001$ (Fisher's exact test)

† $P=0.0028$ (Fisher's exact test)

the CT images of SPECT/CT in 9 of the 11 patients. Only 1 of the 11 patients complained of abdominal muscular pain above the navel, which commenced 24 h after treatment and lasted for 48 hours without any skin changes. This case has been discussed in detail in a recent publication [19]. Neither of the two patients showing tracer accumulation in the spleen developed any relevant side effects. One patient showed a focally increased accumulation in the gallbladder without developing any side effects. The accumulation was detectable only on SPECT/CT images.

Discussion

Although SPECT imaging is normally performed with gamma-emitting radioactive agents, imaging can also be performed using BS, detecting the photons emitted by the beta particles as they lose their energy in the body [11, 21]. Whole-body and planar BS scans can detect diffuse extrahepatic ^{90}Y microsphere accumulations in the lungs, intestinal tract or along the hepatic falciform artery. However, the analysis of BS scans may be difficult and even misleading due to the low spatial resolution. Furthermore, the location of several different organs within a relatively small region in the upper abdomen demands the analysis of tomographic images to accurately distinguish whether the ^{90}Y has accumulated in the liver or in an adjacent organ.

In this study, in order to achieve the best possible sensitivity, we used a very broad energy window of 55–250 keV for the BS acquisitions. We also applied iterative reconstruction in view of the poor image quality of filtered back-projection reconstructed scans.

Of the 188 series of whole-body scans, 12 (6.3%) could not be properly evaluated in our study due to a high level of scatter artefacts and low image quality. SPECT images, on the other hand, showed a high FP rate and therefore were not really suitable for the prediction of GI ulcers (Fig. 4).

BS SPECT/CT showed significantly better sensitivity, specificity, PPV and NPV compared than BS SPECT alone. The PPV of the test was especially of great importance because all patients showing extrahepatic accumulation in the GI region on posttherapy BS SPECT/CT had to receive a higher prophylactic dose of proton pump inhibitors, and underwent diagnostic gastroduodenoscopy as early as possible to avoid any fatal ulcers. It is not clear if some cytoprotective drugs such as amifostine have any protective effect against the development of RE-induced injuries.

To our knowledge, this is the first study examining the performance of BS SPECT/CT after RE with ^{90}Y microspheres compared to BS SPECT and planar imaging considering extrahepatic shunting of microspheres to other abdominal organs as well as its significance in the prediction of RE-induced extrahepatic side effects. A few recent studies and case reports have shown the utility of ^{90}Y-PET in the evaluation of the biodistribution of ^{90}Y microspheres after RE. For this purpose, both iterative and time-of-flight reconstruction methods have been described as feasible [22–26]. A valid measurement of the absorbed

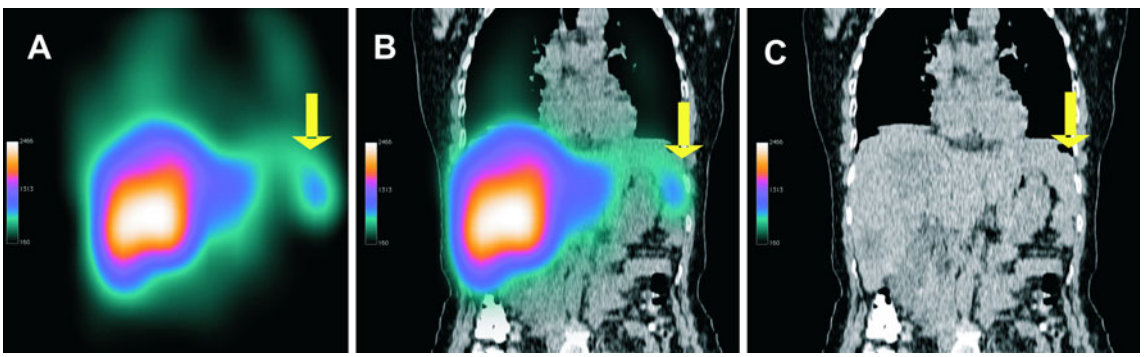

Fig. 4 SPECT alone may not be appropriate as a posttherapy imaging modality in patients undergoing RE due to the high rate of FP findings as in this patient. Tracer accumulation in the left abdomen in the coronal BS SPECT image (*arrows*). **a** SPECT coronal image shows suspicious extrahepatic accumulation which proved to be a hypertrophied left liver lobe after fusion with the CT image (**b** and **c**)

dose is also expected via ^{90}Y PET [24]. Therefore, ^{90}Y PET/CT imaging may potentially be an alternative in this setting when a SPECT/CT camera is not available. However, more studies are needed to determine acceptable reconstruction methods and acquisition parameters [27].

Conclusion

The GI region cannot be evaluated in BS planar or SPECT images. Despite the overall low quality of BS imaging, the use of SPECT/CT makes it a reliable procedure to confirm the safe distribution of ^{90}Y microspheres and for prediction of GI side effects. This may lead to the early planning of an appropriate approach to the treatment of GI side effects.

Conflicts of interest None.

References

1. Murthy R, Nunez R, Szklaruk J, Erwin W, Madoff DC, Gupta S, et al. Yttrium-90 microsphere therapy for hepatic malignancy: devices, indications, technical considerations, and potential complications. Radiographics. 2005;25 Suppl 1:S41–55. doi:10.1148/rg.25si055515.
2. Ahmadzadehfar H, Biersack HJ, Ezziddin S. Radioembolization of liver tumors with yttrium-90 microspheres. Semin Nucl Med. 2010;40:105–21. doi:10.1053/j.semnuclmed.2009.11.001.
3. Riaz A, Lewandowski RJ, Kulik LM, Mulcahy MF, Sato KT, Ryu RK, et al. Complications following radioembolization with yttrium-90 microspheres: a comprehensive literature review. J Vasc Interv Radiol. 2009;29:1121–30. doi:10.1016/j.jvir.2009.05.030.
4. Tehranipour N, AL-Nahhas A, Canelo R, Stamp G, Woo K, Tait P, et al. Concordant F-18 FDG PET and Y-90 Bremsstrahlung scans depict selective delivery of Y-90-microspheres to liver tumors: confirmation with histopathology. Clin Nucl Med. 2007;32:371–4. doi:10.1097/01.rlu.0000259568.54976.bd.
5. Sebastian AJ, Szyszko T, Al-Nahhas A, Nijran K, Tait NP. Evaluation of hepatic angiography procedures and bremsstrahlung imaging in selective internal radiation therapy: a two-year single-center experience. Cardiovasc Intervent Radiol. 2008;31:643–9. doi:10.1007/s00270-008-9298-4.
6. Mansberg R, Sorensen N, Mansberg V, Van der Wall H. Yttrium 90 Bremsstrahlung SPECT/CT scan demonstrating areas of tracer/tumour uptake. Eur J Nucl Med Mol Imaging. 2007;34:1887. doi:10.1007/s00259-007-0536-9.
7. Fabbri C, Sarti G, Cremonesi M, Ferrari M, Di Dia A, Agostini M, et al. Quantitative analysis of 90Y Bremsstrahlung SPECT-CT images for application to 3D patient-specific dosimetry. Cancer Biother Radiopharm. 2009;24:145–54. doi:10.1089/cbr.2008.0543.
8. Minarik D, Sjogreen Gleisner K, Ljungberg M. Evaluation of quantitative (90)Y SPECT based on experimental phantom studies. Phys Med Biol. 2008;53:5689–703. doi:10.1088/0031-9155/53/20/008.
9. Minarik D, Ljungberg M, Segars P, Gleisner KS. Evaluation of quantitative planar 90Y bremsstrahlung whole-body imaging. Phys Med Biol. 2009;54:5873–83. doi:10.1088/0031-9155/54/19/014.
10. Lassmann M. Dosimetry of short-ranged radionuclides. Nuklearmedizin. 2010;49 Suppl 1:S46–9.
11. Walrand S, Flux GD, Konijnenberg MW, Valkema R, Krenning EP, Lhommel R, et al. Dosimetry of yttrium-labelled radiopharmaceuticals for internal therapy: 86Y or 90Y imaging? Eur J Nucl Med Mol Imaging. 2011;38 Suppl 1:S57–68. doi:10.1007/s00259-011-1771-7.
12. Ito S, Kurosawa H, Kasahara H, Teraoka S, Ariga E, Deji S, et al. (90)Y bremsstrahlung emission computed tomography using gamma cameras. Ann Nucl Med. 2009;23:257–67. doi:10.1007/s12149-009-0233-9.
13. Even-Sapir E, Keidar Z, Bar-Shalom R. Hybrid Imaging (SPECT/CT and PET/CT) – improving the diagnostic accuracy of functional/metabolic and anatomic imaging. Semin Nucl Med. 2009;39:264–75. doi:10.1053/j.semnuclmed.2009.03.004.
14. Vermeeren L, Valdes Olmos RA, Meinhardt W, Bex A, van der Poel HG, Vogel WV, et al. Value of SPECT/CT for detection and anatomic localization of sentinel lymph nodes before laparoscopic sentinel node lymphadenectomy in prostate carcinoma. J Nucl Med. 2009;50:865–70. doi:10.2967/jnumed.108.060673.
15. Schmidt D, Szikszai A, Linke R, Bautz W, Kuwert T. Impact of 131I SPECT/spiral CT on nodal staging of differentiated thyroid carcinoma at the first radioablation. J Nucl Med. 2009;50:18–23. doi:10.2967/jnumed.108.052746.
16. Patel CN, Chowdhury FU, Scarsbrook AF. Clinical utility of hybrid SPECT-CT in endocrine neoplasia. AJR Am J Roentgenol. 2008;190:815–24. doi:10.2214/AJR.07.2946.
17. Ahmadzadehfar H, Sabet A, Biermann K, Muckle M, Brockmann H, Kuhl C, et al. The significance of 99mTc-MAA SPECT/CT liver perfusion imaging in treatment planning for 90Y-microsphere selective internal radiation treatment. J Nucl Med. 2010;51:1206–12. doi:10.2967/jnumed.109.074559.
18. Sabet A, Ahmadzadehfar H, Muckle M, Haslerud T, Wilhelm K, Biersack HJ, et al. Significance of oral administration of sodium perchlorate in planning liver-directed radioembolization. J Nucl Med. 2011;52:1063–7. doi:10.2967/jnumed.110.083626.
19. Ahmadzadehfar H, Mohlenbruch M, Sabet A, Meyer C, Muckle M, Haslerud T, et al. Is prophylactic embolization of the hepatic falciform artery needed before radioembolization in patients with (99m)Tc-MAA accumulation in the anterior abdominal wall? Eur J Nucl Med Mol Imaging. 2011;38:1477–84. doi:10.1007/s00259-011-1807-z.
20. MDS Nordion. TheraSphere® Yttrium-90 Glass Microspheres: instructions for use, Ottawa: MDS Nordion. http://www.nordion.com/therasphere/physicians-package-insert/package-insert-eu-en.pdf. Accessed 28 Sep 2011.
21. D'Asseler Y. Advances in SPECT imaging with respect to radionuclide therapy. Q J Nucl Med Mol Imaging. 2009;53:343–7.
22. Gates VL, Esmail AA, Marshall K, Spies S, Salem R. Internal pair production of 90Y permits hepatic localization of microspheres using routine PET: proof of concept. J Nucl Med. 2011;52:72–6. doi:10.2967/jnumed.110.080986.
23. Lhommel R, Goffette P, Van den Eynde M, Jamar F, Pauwels S, Bilbao JI, et al. Yttrium-90 TOF PET scan demonstrates high-resolution biodistribution after liver SIRT. Eur J Nucl Med Mol Imaging. 2009;36:1696. doi:10.1007/s00259-009-1210-1.
24. Lhommel R, van Elmbt L, Goffette P, Van den Eynde M, Jamar F, Pauwels S, et al. Feasibility of 90Y TOF PET-based dosimetry in liver metastasis therapy using SIR-Spheres. Eur J Nucl Med Mol Imaging. 2010;37:1654–62. doi:10.1007/s00259-010-1470-9.
25. Werner MK, Brechtel K, Beyer T, Dittmann H, Pfannenberg C, Kupferschlager J. PET/CT for the assessment and quantification

of (90)Y biodistribution after selective internal radiotherapy (SIRT) of liver metastases. Eur J Nucl Med Mol Imaging. 2010;37:407–8. doi:10.1007/s00259-009-1317-4.
26. Wissmeyer M, Heinzer S, Majno P, Buchegger F, Zaidi H, Garibotto V, et al. (90)Y Time-of-flight PET/MR on a hybrid scanner following liver radioembolisation (SIRT). Eur J Nucl Med Mol Imaging. 2011;38:1744–5. doi:10.1007/s00259-011-1792-2.
27. Ahmadzadehfar H, Sabet A, Reichmann K, Muckle M, Habibi E, Biersack H, et al. Imaging of Y90 distribution with PET/CT and bremsstrahlung SPECT/CT after radioembolization: A patient based study. J Nucl Med. 2011;52 Suppl 1. Abstract 92